Nanoscale

Accepted Manuscript

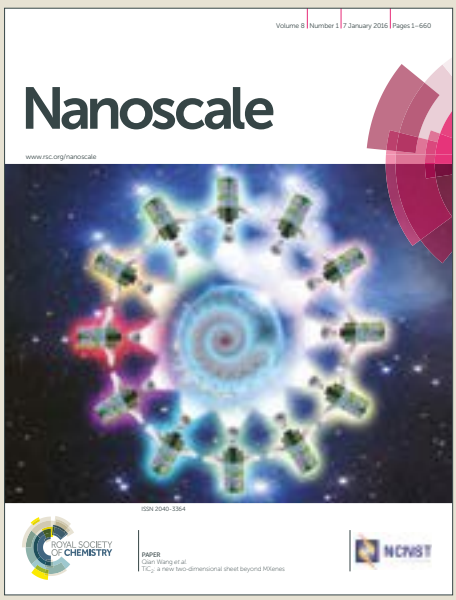

ROYAL SOCIETY OF CHEMISTRY

rsc.li/nanoscale

View Article Online
DOI: 10.1039/C7NR03754F

The interaction of photoexcited Carbon nanodots with metal ions disclosed down to the femtosecond scale.

A. Sciortino[1,2,3], A. Madonia[1], M. Gazzetto[3], L. Sciortino[1], E. J. Rohwer[3], T. Feurer[3], F. M. Gelardi[1], M. Cannas[1], A. Cannizzo[3,*], F. Messina[1,4,**]

[1]Dipartimento di Fisica e Chimica, Università degli Studi di Palermo, Via Archirafi 36, 90123 Palermo, Italy.
[2]Dipartimento di Fisica e Astronomia, Università degli Studi di Catania, Via Santa Sofia 64, 95123 Catania, Italy.
[3]Institute of Applied Physics, University of Bern, Sidlerstrasse 5, CH-3012 Bern, Switzerland.
[4]CHAB – ATeN Center, Università degli Studi di Palermo, Viale delle Scienze, Edificio 18, 90128 Palermo, Italy
*andrea.cannizzo@iap.unibe.ch **fabrizio.messina@unipa.it,

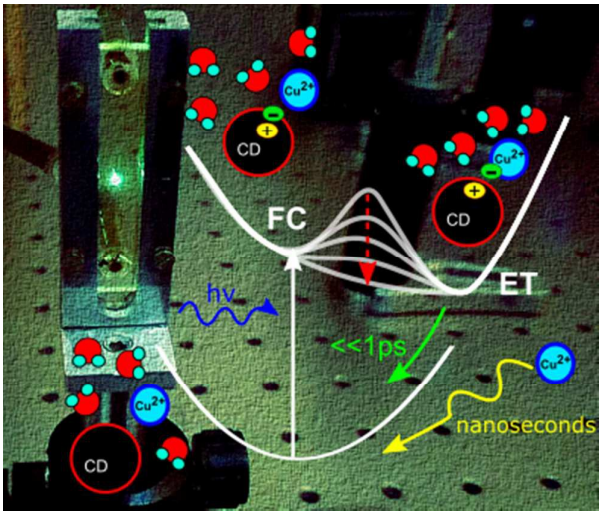

We use a combination of steady-state, nanosecond-resolved, and femtosecond-resolved optical spectroscopies to fully unravel the interactions of highly fluorescent Carbon nanodots with transition metal ions.

Abstract

Fluorescent Carbon nanodots are a novel family of carbon-based nanoscale materials endowed with an outstanding combination of properties that make them very appealing for applications in nanosensing, photonics, solar energy harvesting and photocatalysis. One of the remarkable properties of Carbon dots is their strong sensitivity to local environment, especially to metal ions in solution. These interactions provide a testing ground of their marked photochemical properties, highlighted by many studies, and frequently driven by charge transfer events. Here we combine several optical techniques, down to the femtosecond time resolution, to understand the interplay

View Article Online
DOI: 10.1039/C7NR03754F

between Carbon nanodots and aqueous metal ions such as Cu^{2+} and Zn^{2+}. We find that copper inhibits the fluorescence of carbon dots through static and diffusional quenching mechanisms, and our measurements allow discriminating between the two. Ultrafast optical methods are then used to address the dynamics of copper-dot complexes, wherein static quenching takes place, and unveil the underlying complexity of their photocycle. We propose an initial increase of electronic charge on the surface of the dot, upon photo-excitation, followed by a partial electron transfer to the nearby ion, with 0.2 ps and 1.9 ps time constants, and finally a very fast (<<1 ps) non-radiative electron-hole recombination which brings the system back to the ground state. Notably, we find that the electron transfer stage is governed by ultrafast water rearrangement around photo-excited dots, pointing out the key role of solvent interactions in the photo-physics of these systems.

Introduction

Carbon Nanodots (CDs) are a recent class of nanomaterials which have received a great attention in the broad world of nanoscience since their accidental discovery in 2004. [1] The large interest for these systems may be mostly attributed to their fascinating photoluminescence, [2] uncommon in C-based nanoscale materials, usually tunable throughout the visible range, and highly sensitive to the environment or to interactions with external agents. Moreover, CDs combine these remarkable fluorescent capabilities with an apparent lack of toxicity, [3] high water solubility, [4] and easy synthesis procedures. [5]

The use of CDs in nano-sensing applications has been intensively studied as one of their most interesting applications. CDs are highly responsive to the presence of metal ions in solution, whereby many works reported a variation (quenching or enhancement) of their luminescence in presence of different types of ions. [6-13] Depending on the surface structure of CD, these interactions can be very selective and reversible. For instance, Zhang *et al.* reported an interaction between CDs and Fe^{3+} ions, and the consequent quenching of CD emission, already at nanomolar iron concentrations, [9] while Zhong et al. showed how the fluorescence of CDs is turned off when they contact Cu^{2+} ions, and how is turned back on by addition of L-cysteine, which detaches the ions from the dot surface. [8] The most popular explanation of these quenching phenomena invokes an efficient electron transfer from CDs to metal ions or molecules, which hinders the radiative recombination of the photo-generated excitons.[14] Interestingly, some works have suggested that these CD-metal quenching interactions are influenced by the solvent, [14] suggesting a role of solvation in the underlying photochemical interactions.

As a matter of fact, the ability of CDs to act as efficient photo-activated electron acceptors or donors is rather well-established and not limited to the interaction with transition metal ions. These

View Article Online
DOI: 10.1039/C7NR03754F

photochemical properties of CDs are regarded as one of their most interesting hallmarks because of their impact in the design of several types of functional hybrid nanoscale systems. For instance, similar charge transfer dynamics are observed between CDs and metal complexes [15], or when CDs are adsorbed on semiconductor surfaces [16] and may allow to use them as green substitutes of metal-complexes to harvest solar energy in dye-sensitized solar cells (DSSC), [17] or to strongly enhance the photocatalytic activity of semiconductor nanoparticles such as TiO_2, Cu_2O, Fe_2O_3. [18-22] Understanding these photochemical interactions of CDs is of crucial importance to optimize potentially far-reaching applications, and may provide precious information on the very nature of CDs electronic transitions. In fact, there are still several open questions about the emission process of CDs, especially in regard to the interplay between core- and surface-related electronic states. We recently proposed [23] that the lowest-energy optical transitions of CDs involve an increase of the electronic charge on surface functional groups at the expense of nearby core atoms. This indicates a transition typified by a certain charge separation character. Because of this, the surface electron should be especially prompt to participate to charge transfer dynamics, possibly explaining the strong interactions of CDs with metal ions. Actually, charge transfer processes involving semiconductor quantum dots are often mediated by their surface groups. [24]

We carried out a study aimed to thoroughly clarify the interactions between photo-excited CDs and metal ions in solution, using Cu^{2+} as a model system. If electron transfer dynamics are implicated in these interactions, Cu^{2+} should be a very good candidate to clarify them, considering its open-shell electronic configuration ($[Ar]3d^9$), the fairly positive redox potential, and the fact that its absorption spectrum does not overlap with either the absorption or the emission bands of CDs. Since fluorescence quenching often occurs over extremely short time scales (picoseconds or less [25]), the use of femtosecond-time-resolved spectroscopies is mandatory to observe these events in real time. Up to now, studies of CDs with sub-picosecond optical spectroscopy are still rare. [26-28]

In our study, we find that CD fluorescence is quenched by Cu^{2+} ions through a combination of dynamic and static quenching mechanisms. While the former are due to collisional encounters related to the high concentration of ions, the latter arise from the formation of CD/Cu^{2+} complexes, whereby our results suggest a single Cu^{2+} ion binding to the dot surface is enough to quench its emission. Interestingly, the static and dynamic quenching rates are affected by significant dot-do-dot variations related to the heterogeneity of the system, leading to photoselection effects. Most importantly, by resolving in time the photocycle of CD/Cu^{2+} complexes, our experiments unveil the ultrafast, characteristic mechanism and ultrafast time scale of fluorescence quenching events. The emissive electron-hole pair generated by photo-excitation gets decoupled by a partial electron transfer towards the ion, followed by a remarkably fast (<< 1 ps) non-radiative electron-hole

View Article Online
DOI: 10.1039/C7NR03754F

recombination, which concludes the photocycle. Furthermore, we demonstrate that the electron transfer is controlled by picosecond and sub-picosecond solvent rearrangements around the photo-excited site, progressively lowering the reaction barrier. In this sense, solvent molecules are a vital component of the photochemical behavior of CDs, rather than spectators.

Experimental Section

Sample preparation and characterization

The synthesis of CDs was carried out by the microwave-induced hydrothermal decomposition of an aqueous solution of citric acid and urea, in a 1:1 weight ratio. Urea is added in the synthesis as a source of Nitrogen doping in order to enhance the optical properties of the nanomaterial. The synthesis procedure and the successive characterization of these nanomaterials by high-resolution transmission electron microscopy, electron diffraction, atomic force microscopy, X-ray photoelectron spectroscopy, and Fourier-transform infrared absorption was described in detail in a previous work.[29] Shortly, these CDs are 3 nm-sized carbon nitride nanocrystals, surface-functionalized with amide and carboxylic groups. [29]

Steady-state and nanosecond time-resolved optical measurements

All the solutions measured here by steady-state optical techniques and time-resolved fluorescence were prepared by dissolving a 8 mg/L concentration of CDs in milliQ water, together with different amounts of $Cu(NO_3)_2$, $CuSO_4$ or $ZnSO_4$ (Sigma-Aldrich). All measurements were carried out at room temperature. The absorption spectra were recorded by a double beam spectrophotometer (JASCO V-560) in the 220-750 nm range in a 1 cm quartz cuvette. The emission spectra were recorded with a JASCO FP-6500 spectrofluorometer in a 1 cm cuvette Infrared absorption spectra were recorded on a N_2-purged, Bruker VERTEX-70 spectrophotometer, in transmission geometry. The measurements were performed at room temperature under Nitrogen flux to eliminate the effect of residual water in the air. Samples were prepared by depositing drops of a CDs + $Cu(NO_3)_2$ solution on a sapphire window and drying in vacuum. Time-resolved fluorescence measurements were achieved by a tunable laser system consisting in an optical parametric oscillator pumped by a Q-switched Nd:YAG laser (5 ns pulses at 10 Hz repetition rate). Fluorescence spectra were recorded on an intensified charge coupled device (CCD) camera, integrating the signal within temporal windows of 0.5 ns duration after variable delays from the laser pulse. The obtained decay kinetics of the photoluminescence were least-squares fitted to exponential functions convoluted with a Gaussian instrumental response function (IRF) with a 5 ns

View Article Online
DOI: 10.1039/C7NR03754F

full width at half maximum (FWHM), determined by the laser temporal profile. The accuracy on the time constant of the decays is about 0.2 ns.

Femtosecond-resolved transient absorption

The broadband femtosecond transient absorption (TA) measurements on the solution of pure CDs in water and ethanol, and on CDs+100mM Cu^{2+} in water were based on a 1 kHz Ti:Sapphire regenerative amplifier system which generates 90 fs pulses centered at 800 nm with 0.8 mJ pulse energy. The beam is split to generate pump and probe beampaths. The pump passes through an ultrathin BBO (Beta Barium Borate) crystal where it is frequency-doubled to produce the excitation at 400 nm, which is then chopped at the repetition rate of 500 Hz, synchronized with the regenerative amplifier output. For probing, a referenced broadband detection scheme is adopted. A white light pulse (350 to 700 nm) is generated by focusing a fraction of the fundamental in a 5 mm-thick CaF_2 crystal. Then it is split in two identical beams: one (the probe) is overlapped with the pump in the sample, the other (the reference) is sent through an unpumped volume of the sample to correct for white-light fluctuations on a single shot basis. The pump-probe delay t is controlled by a motorized delay stage. Pump and probe are synchronously collected with a multi-camera detector system (Glaz Linescan-I) with single-shot capability. The spectrum of probe and reference pulses are measured on a single-shot basis, and successive pumped and unpumped probe shots (due to the chopper) are compared to correct for drift of transmission baseline over time. This is used to calculate the TA signal, that is the change $\Delta OD(\lambda,t)$ in the absorption of the sample induced by photo-excitation. A typical signal is obtained by averaging 1000 pumped and 1000 unpumped spectra for each delay, and scanning over the pump-probe delay 4-5 times.

The single-wavelength TA measurements and the broadband measurement on the solution of CDs+30 mM Zn^{2+} are based on a 5 kHz Ti:Sapphire femtosecond ultrafast amplifier (Solstice-Ace) which generates 50 fs pulses at 800 nm with 0.7 mJ energy, split (80%/20%) to generate the pump and the probe. Also in this setup, the pump beam is frequency-doubled by an ultrathin BBO crystal in order to create a 400 nm beam which is then chopped at 500Hz, whereas the white light beam is generated in a 2 mm quartz cuvette containing D_2O, generating a broadband pulse extending from 400 to 700 nm. After overlapping with the pump within the sample, the probe beam is dispersed on the detector through a Brewster-angle silica prism and the measurement wavelength is selected by a variable slit, which guarantees a spectral resolution of 3 nm at 550 nm. The detector used for the single-wavelength measurements is a photomultiplier connected to a lock-in amplifier. The latter, triggered by the chopper, allows to extract the TA signal as the component of the probe signal locked to the chopper frequency. A typical signal is obtained by scanning 10 times the pump/probe

View Article Online
DOI: 10.1039/C7NR03754F

delay, and using an integration time of 1.5 s per point. The obtained time traces were least-squares fitted to multi-exponential functions convoluted with the Gaussian IRF of the setup, having a FWHM=120 fs. For the broadband measurement performed in this setup, the detector is the multi-camera system (Glaz Linescan-I) illustrated above.

The broadband and the single-wavelength measurements are collected at room temperature in the same conditions. The solutions were prepared by adding the same amount of CDs (final concentration of about 1.2 g/L), and were continuously circulated in a 0.2 mm thick flow cell, in order to have an absorbance value of 0.3 OD at 400 nm. The measurements were performed in linear regime with energy of about 100 nJ/pulse and we checked that the signal was not concentration dependent. All measurements were carried out in, so-called, magic angle detection conditions, such that they are not affected by rotational diffusion or depolarization dynamics. The data presented in the paper were subjected to standard correction procedures which eliminate the effects of cross-phase modulation (XPM) and group velocity dispersion (GVD).

Results and Discussion

1. Effect of metal ions on CD fluorescence: static and dynamic quenching.

CDs were synthesized by a single-step procedure based on microwave-induced decomposition of citric acid and urea. As reported in greater detail in ref. [29], the core of these CDs has a carbon nitride crystalline structure and their surface shell is rich of carboxylic and amide groups. We show in Figure 1a their electronic absorption spectrum, peaking around 400 nm (purple spectrum). We dispersed a given amount of dots in water, together with different amounts of Cu^{2+} ions, and studied how their optical properties change with the increase of ion concentration. Figure 1b displays the steady state emission spectra excited at 440 nm of an aqueous solution of CDs (8 mg/L) and variable concentrations of copper nitrate. It is evident that the photoluminescence is quenched by the ions, similar to previous reports in the literature. [8] Since effects in Figure 1 are essentially independent of the counter ion (Figure S1 in the electronic supplementary information - ESI), quenching can be safely attributed to the interaction with aqueous Cu^{2+}. In the inset of Figure 1b, we report how the luminescence intensity decreases with increasing $[Cu^{2+}]$: appreciable variations of the emission intensity are observed already at concentrations as low as 2 μM, where we detect a $\Delta I/I_0 \approx 10\%$ reduction, and a very marked quenching is observed when copper concentration reaches the millimolar range, with a $\Delta I/I_0 \approx 50\%$ loss of the luminescence efficiency recorded at $[Cu^{2+}]$=2 mM. We also see a blueshift of the band from 525 nm down to 512 nm, measured at $[Cu^{2+}]$=500

View Article Online
DOI: 10.1039/C7NR03754F

mM together with an intensity reduction of $\Delta I/I_0 \approx 96\%$. We also investigated the effect of Cu^{2+} ions on the steady state absorption properties: as shown in Figure 1a, the addition of metal ions causes an intensity reduction and a blueshift (>20 nm when $[Cu^{2+}]$=500 mM) of the absorption band at 400 nm.

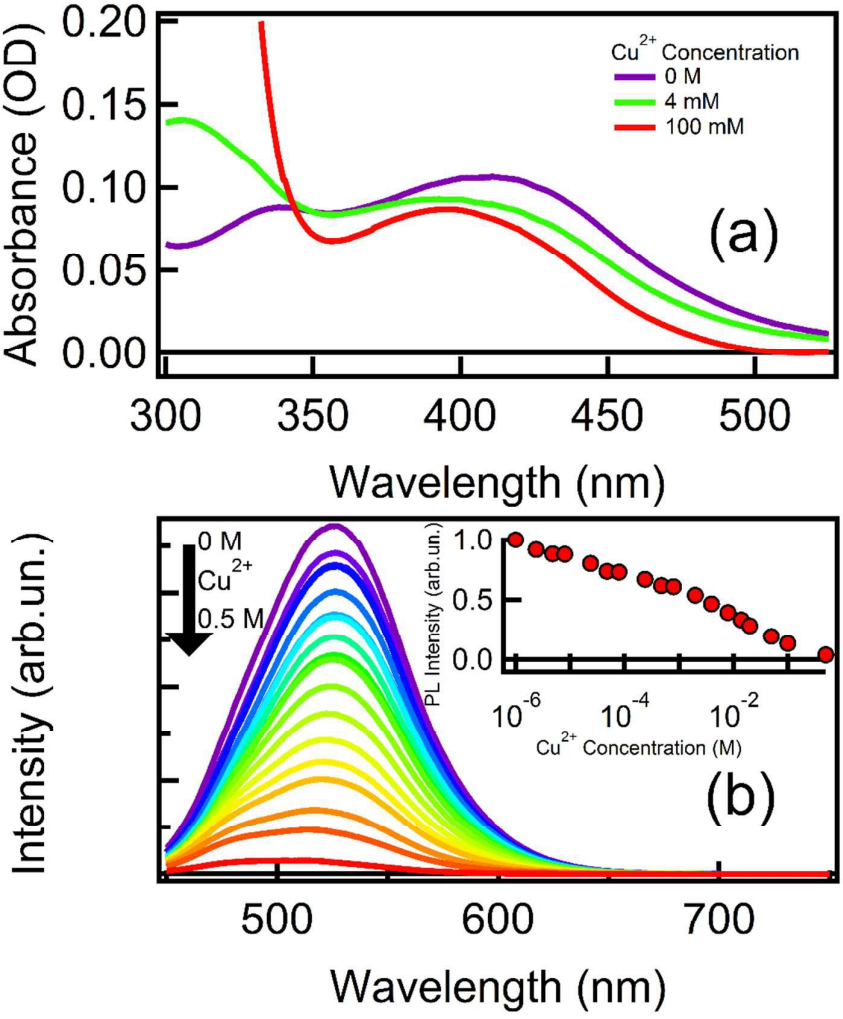

Figure 1: *(a): Selected absorption spectra of CDs as measured in the presence of different Cu^{2+} concentrations. The edge below 350 nm is due to electronic transitions of the counterion (NO_3^-). (b): Steady-state emission spectra excited at 440 nm of CDs dissolved in water together with Cu^{2+} ions in concentrations ranging from zero to 500 mM (increasing along the arrow). Inset: Photoluminescence intensity, normalized to bare CDs, versus Cu^{2+} concentration. Selected values are reported in Table I.*

We performed nanosecond time-resolved fluorescence measurements (Figure 2 and Table 1), in order to disentangle static and dynamic quenching mechanisms. In Figures 2a-b, we show the 2-

View Article Online
DOI: 10.1039/C7NR03754F

dimensional (2D) time-wavelength plots of the fluorescence intensity of the bare CDs solution and of bare CDs + 50 mM copper ions excited at 440 nm, respectively. The photoluminescence decay kinetics at fixed emission wavelength, such as those in Figure 2c, are obtained by a vertical cut of the 2D-plot and the emission spectra at fixed time are obtained by a horizontal cut of the same plot and then normalized, as in Figure 2d. The decay kinetics of bare CDs are single-exponential, with a lifetime of τ_0=6.2 ns, and displays no spectral evolution. We find that diffusion-controlled (i.e. dynamic) quenching comes into play only above a certain Cu^{2+} concentration, as revealed by a decrease of the lifetime: we detect the first deviations of the fluorescence kinetics at [Cu^{2+}]=20 mM (green curve in Figure 2c, τ_0=5.0 ns), and the lifetimes continue decreasing at higher quencher concentrations down to <2.0 ns. In presence of copper, at fixed concentrations, we also see that a blueshift of the band occurs during the decay, as shown in Figure 2d. In fact, the lifetime becomes slightly emission-dependent: as shown in Figure S2, the lifetimes of the emission band when [Cu^{2+}]=50 mM span from 3 ns (emission wavelength 490 nm) to 4.6 ns (600 nm).

However, such a diffusion-controlled mechanism cannot explain the quenching observed at millimolar concentrations and lower, when the probability of collisions between diffusing Cu^{2+} and CDs during the excited-state lifetime is negligible. This is evident if we consider the significant quenching observed at extremely low concentrations: considering the typical bimolecular diffusion-limited reaction rates in water ($K\approx10^{10}$ $M^{-1}s^{-1}$), [30] the expected quenching I/I_0 due to collisions can be roughly estimated as $(1+\tau_0 K[Cu^{2+}])^{-1}$. For [$Cu^{2+}$]=2 μM, this only gives $\Delta I/I_0=5\cdot10^{-5}$, several orders of magnitude less than we observe ($\Delta I/I_0\approx10\%$, as from Figure 1). In fact, as previously reported for other CDs, [12] we find that the lifetime is unchanged (τ=5.9 ns, blue and light blue datasets in Figure 2c) up to [Cu^{2+}] = 4 mM, although the emission intensity decreases twofold (as from Figure 1b). More fundamental, a decrease of the amplitude without shortening of the lifetime can only be explained by the presence of non-radiative channels affecting the excited state population on time scales much shorter than the time resolution. On these time scales the mechanism cannot be diffusional and it points to a mechanism where copper ions are in interaction with the dots before and during photoexcitation.

Hence the quenching is purely static, i.e. occurring without collisions, up to millimolar Cu^{2+} concentrations: ground-state interactions between CDs and Cu^{2+} ions lead to the formation of weakly, or non-luminescent CD-Cu^{2+} complexes. As observed in Figures 1 and 2 for [Cu^{2+}] = 4 mM, in this regime the emission keeps the same lifetime and spectral characteristics, as expected for static quenching, because the observed steady-state fluorescence only arises from the remaining, uncomplexed dots. In contrast, both bare CDs and CD-Cu^{2+} complexes contribute to the absorption spectrum, and changes are observed (Figure 1a). The observed intensity reduction of the absorption

View Article Online
DOI: 10.1039/C7NR03754F

band indicates a significant perturbation of the electronic wavefunction, clearly demonstrating the close proximity of Cu^{2+} ions on the surface of CDs. The absorption blueshift possibly arises from electrostatic screening of CD-Cu^{2+} complexes, hampering solvent-induced stabilization which usually redshifts CD transitions. [31] Also a ground state stabilization effect is very likely: from the very fact that the formation of CD-Cu^{2+} complexes occurs spontaneously, Cu^{2+} atoms bonding to the surface to the dots are expected to stabilize their ground-state energy, leading to a blueshift in the OA spectra. Another interesting information that can be inferred from the absorption spectra is that the latter continue to evolve even above the onset (≈10 mM) of dynamic quenching, suggesting a continuous increase of static effects up to the largest quencher concentrations we explored. We use the equation $I/I_0=(1-f)(\tau/\tau_0)$ to estimate the portions of CD population which undergo static (*f*) and dynamic (1-*f*) quenching. At the maximum copper concentration ($[Cu^{2+}]$=500 mM) we explored, I/I_0=0.05 and τ=1.5 ns, corresponding to *f*=80%, indicating static quenching is always dominant.

Finally, from the inset of Figure 1b, another interesting effect is that the quenching effect is spread across the entire concentration range we explored. The response to copper of the emission intensity is very broad both in the static and dynamic quenching concentration ranges. This behavior suggests a broad distribution of both the reaction rates, fluctuating from dot to dot. The distribution of the static quenching rate may arise from different surface structures of the dots corresponding to different association rate constants with Cu^{2+} ions, while the distribution of the dynamic rate is probably due to different capture radii, linked to different size of the dots. Such an heterogeneous response of different CDs to Cu^{2+} ions should give rise to photoselection effects, explaining both the blueshift of the steady-state fluorescence at high Cu^{2+} concentrations in Figure 1b (red-emitting dots have larger association constants and are the first to undergo static quenching) and the emission-dependence of the lifetime in Figure S2 (red-emitting dots have larger capture radii for diffusing Cu^{2+} ions, hence shorter lifetimes).

View Article Online
DOI: 10.1039/C7NR03754F

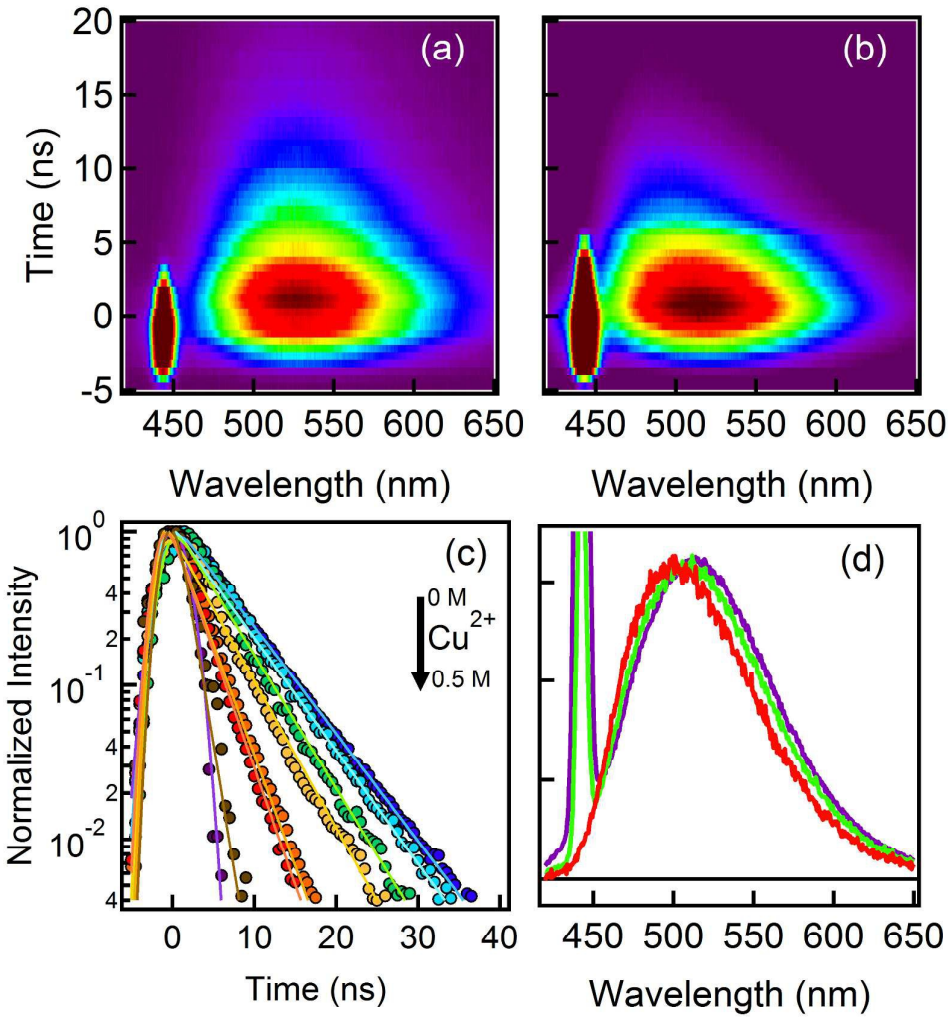

Figure 2: *Fluorescence 2-dimensional plots of bare CDs in water excited at 440 nm (a), and with a Cu^{2+} concentration of 50 mM (b); the feature at 440 nm is the excitation laser pulse. (c): Normalized decay fluorescence of CDs excited at 440 nm in water with zero (blue markers), 4 mM (light blue markers), 20 mM (green markers), 50 mM (yellow markers), 100 mM (orange markers), 200 mM (red markers), 500 mM (brown markers) concentration of copper ions, together with the laser pulse (purple markers),with the respective least-squares fitting curves. (d): Normalized emission spectra recorded for $[Cu^{2+}]$=50 mM at different times: 2.5 ns (purple), 5 ns (green) and 7.5 ns (red).*

View Article Online
DOI: 10.1039/C7NR03754F

Table 1: *Summary of the characteristic time scales and amplitudes of the kinetics from Figure 2c and Figure 4a at representative concentrations of Cu^{2+} ions.*

Concentration	**Normalized Integral of Steady State Emission**	**Fluorescence decay lifetime (ns)**	**TA Decay Amplitudes (mOD)**		
$[Cu^{2+}]$ (mM)			τ_1=0.21± 0.05 ps	τ_2 =1.9±0.1 ps	$\tau_3 \geq$1000 ps
			A_1	**A_2**	**A_3**
0	1.00	6.2 ± 0.2	2.00	1.07	-3.57
4	0.62	5.9 ± 0.2	1.60	0.40	-2.64
20	0.28	5.0 ± 0.2	0.69	-0.12	-1.19
50	0.20	4.6 ± 0.2	0.77	-0.42	-0.87
100	0.13	3.0 ± 0.2	0.66	-0.66	-0.61
200	0.11	2.9 ± 0.2	0.30	-0.59	-0.37
500	0.04	1.5 ± 0.2	0.21	-0.56	-0.19

2. Sub-nanosecond fluorescence quenching induced by Cu^{2+}

The dependence of fluorescence quenching on metal ion content and the mono-exponential ns decay at any concentration, definitively points to the involvement of picosecond or even sub-picosecond deactivation mechanisms. Therefore, we performed femtosecond transient absorption (TA) measurements on aqueous solutions of carbon nanodots with different content of copper ions, excited by 90 fs pulses at 400 nm. We collected broadband TA measurements on an aqueous solution of bare CDs, and on a solution of CDs with $[Cu^{2+}]$=100 mM. The data are shown as time-wavelength 2D-plots in Figures 3a and 3b. The spectra at selected times, such as those in Figure 3c-d and Figure S3, are obtained by vertical cuts of the 2D-plot.

In bare CDs, data at all delays show three contributions to the TA signal: (i) a negative contribution around the pump wavelength, mostly due to ground state bleaching (GSB) associated to the depopulation of the ground state via photo-excitation, with the possible addition of a stimulated emission due to a fluorescence signal peaking at 420 nm (ii) a strong stimulated emission (SE) at 520-550 nm, corresponding to an ordinary fluorescence signal except for its negative sign, and (iii) several positive excited state absorption (ESA) signals, at λ<400 nm, λ~470 nm, and λ>600 nm, respectively, due to electronic transitions from the excited state towards higher excited states. We observe spectral evolution only in the first picoseconds, which mainly consists of a dynamical Stokes shift of the SE signal from 520 nm to 554 nm (Figure S3). Afterwards, no further dynamics are observed. As shown in Figure 3b and 3d, the shape of the signal in presence of Cu^{2+} is

View Article Online
DOI: 10.1039/C7NR03754F

almost the same as bare CDs. However, in the presence of Cu^{2+}, all the components of the signal undergo a decay over a time scale of a few picoseconds, which is not observed for bare CDs.

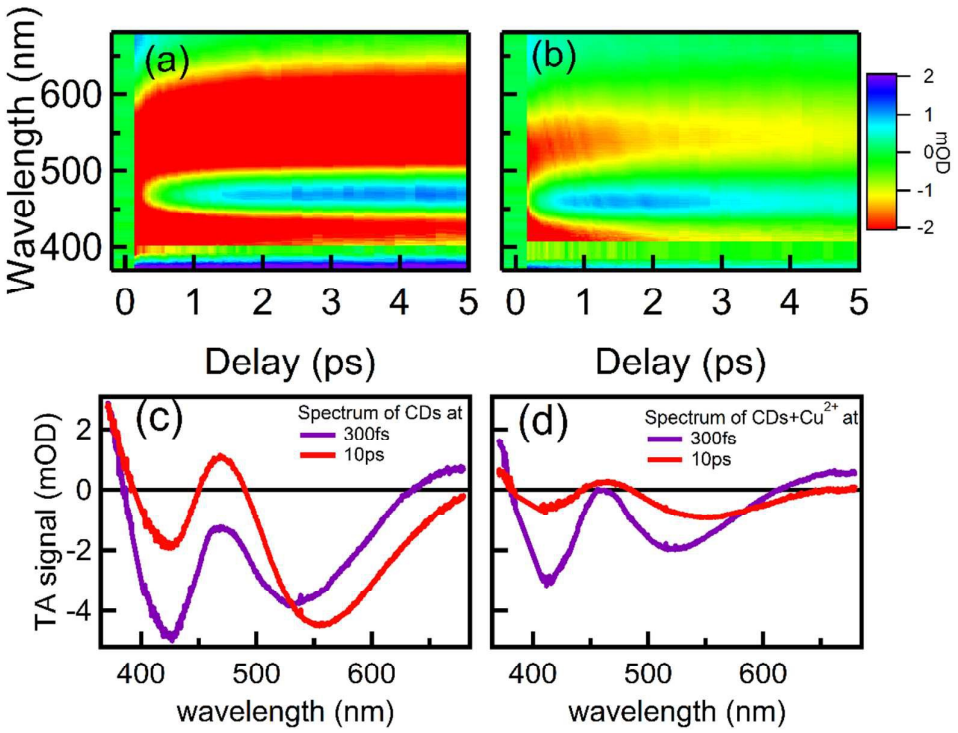

Figure 3: *Transient absorption 2D-plot of an aqueous solution of bare CDs (a) and with [Cu^{2+}]=100 mM (b) excited at 400 nm. Transient absorption spectra of bare CDs (c) and with 100 mM of Cu^{2+} (d) recorded at 300 fs and 10 ps after photoexcitation, as obtained by vertical cuts of the 2D-plots in panels (a) and (b). Data between 388 nm and 405 nm were removed because of distortions by pump scattering around 400 nm.*

View Article Online
DOI: 10.1039/C7NR03754F

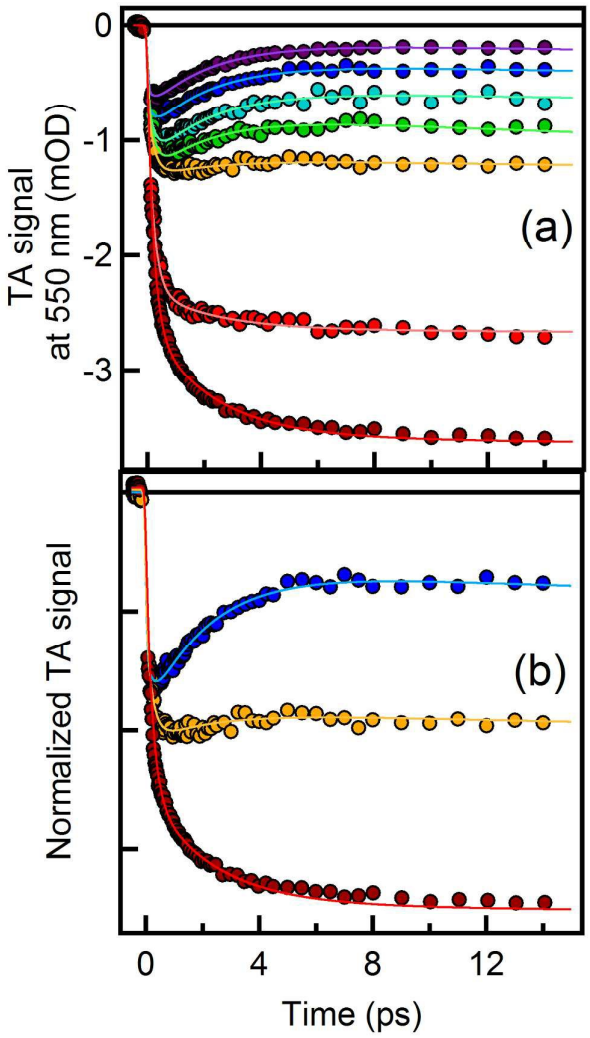

Figure 4: *(a): Transient absorption time traces at 550 nm (excitation at 400 nm) of CDs with no copper ions in solution (dark red), 4 mM (red), 20 mM (orange), 50 mM (green), 100 mM (light blue), 200 mM (blue), 500 mM (purple) copper concentrations, with the respective least-squares fitting curves (continuous lines). (b): Three time traces normalized at the first point after time zero, same color scale.*

Evidently the main effect of metal ions is to alter the overall evolution, but with minimal effect of the spectral features of the TA bands, and single-wavelength kinetic traces can report on the effect of metal-ions on the different spectral components. In order to study the effects of copper ions on the fluorescence, we recorded the SE signal in single-wavelength detection mode to achieve a higher signal-to-noise ratio.

Time traces in Figure 4 were collected at the wavelength of 550 nm close to the peak position of the SE after 10 ps (Figure 3 and Figure S3), to monitor specifically contributions to the SE and thus

View Article Online
DOI: 10.1039/C7NR03754F

excited-state relaxations of CDs. As shown in Figure 4, the signal of bare dots undergoes a rise (i.e. it grows in absolute value) within few ps after photo-excitation. This rise is dominated by the ultrafast dynamical Stokes shift of the entire SE band, which actually peaks at 550 nm after few ps (Figure S3). In presence of Cu^{2+} we see a strong reduction of the SE, similar to Figure 3c. In particular, we observe a decay component over a time scale of a few ps, becoming more and more evident with increasing ion concentration (Figure 4b). We analyzed the single-wavelength kinetics at 550 nm by least-squares fitting all the traces in Figure 4a with multi-exponential functions. We found that every trace can be reproduced by three different time components, τ_1 τ_2 and τ_3. Although the amplitudes associated to these three timescales depend on copper concentration, the timescales obtained by the fit procedure show indeed little variations across the different traces in Figure 4a, and we discovered that all the traces can be simultaneously fitted by common time constants: their values, as obtained by the fit, are τ_1=0.21±0.05 ps, τ_2=1.9±0.1 ps, $\tau_3 \geq$1000 ps, and their amplitudes A_i are reported in Table 1. Being the SE signal negative, a positive (negative) pre-exponential amplitude respectively indicates a rise (decay) of the absolute signal intensity over the corresponding time scale.

The τ_3 component can be identified with the nanosecond-lived fluorescence analyzed in Figures 1 and 2, that is the fluorescence surviving after all the ultrafast dynamics are completed: in fact, increasing [Cu^{2+}] reduces its weight A_3 (see Table 1) similarly to the intensity decrease observed in the inset of Figure 1b. Measurements on an extended delay range (Figure S4) confirm that there is no evolution on the tens and hundreds of picosecond range. This result underscores again that the picosecond (Figure 4) and nanosecond (Figure 2) fluorescence decays induced by addition of Cu^{2+} are well separated, and associated to different processes (static and dynamic quenching, respectively).

The most important information can be drawn, however, by examining the fastest τ_1 and τ_2 dynamics. For bare CDs, the SE signal probed at 550 nm undergoes a bi-exponential rise over two time scales of 0.21 ps and 1.9 ps (A_1 and A_2 positive). In agreement with the previous discussion, the rise is due to the observed dynamical Stokes shift of the SE band (Figure S3) caused by solvation dynamics, that is the relaxation of water around a new electronic distribution impulsively produced by CD photo-excitation. [32] In fact, we certainly expect a significant solvent-induced relaxation of the emission for these CDs, because of their strong fluorescence solvatochromism we recently demonstrated.[23] Because the only SE Stokes shift we observe occurs on the 0.21 and 1.9 ps time scales, and no further spectral evolution is detected up to the nanosecond ranges, these ps and sub-ps dynamics must undoubtedly be attributed to solvation. Furthermore, attributing these processes to solvation is further strengthened by TA data in Figure S5 in which we compare the

View Article Online
DOI: 10.1039/C7NR03754F

aqueous spectra with those recorded in ethanol at the same delays: in ethanol, having a lower polarity, the SE signal is blueshifted and the dynamical Stokes shift is smaller. Observing so strong solvent-dependent effect also confirms that the electronic transition involves the surface, directly exposed and strongly influenced by the solvent. The solvation time scales of CDs have not been systematically investigated by previous studies. A previous work proposed extremely slow solvation at CD surfaces, extending to the nanosecond scale. [33] However, the present results show that CD solvation is actually more similar to that of small molecules or small inorganic nanoparticles,[34] usually very fast and occurring on few ps and sub-ps timescales.[35] In this sense, the hydration layer around CDs is very different from other colloids such as proteins,[36] whose hydration dynamics are significantly slowed down with respect to bulk water.

We discuss now the effect of copper on the dynamics of CDs. The addition of Cu^{2+} decreases the weight of the first rise (τ_1=0.21 ps) and converts the τ_2=1.9 ps rise into a decay, as seen from the change of sign of its amplitude A_2. The ultrafast decay τ_2 directly represents a real-time observation of diffusion-free, static quenching events, which we previously inferred by indirect means. Although the CD-Cu^{2+} complexes involved in these decays are seen as "non-emissive" by steady-state and nanosecond methods, they actually yield a transient fluorescence: in fact, the SE observed in the presence of Cu^{2+} is very close to bare CDs, except for the ultrafast decay (Figure 3). Therefore, CD-Cu^{2+} fluorescence must be observed by ultrafast methods, since it gives essentially no contribution to steady state emission (its quantum yield is $\approx 1\ ps/t_R \leq 10^{-4}$, where $t_R \approx 30$ ns is the radiative lifetime of CDs). [23] Although the amplitude A_1 of the fastest (0.21 ps) component never becomes negative, also its trend can be understood on the same grounds: A_1 becomes smaller with increasing [Cu^{2+}] because the contribution of bare CDs (positive A_1, rise due to solvation) overlaps with the growing contribution of CDs-Cu^{2+} complexes (negative A_1, decay). Overall, these data demonstrate that close-range CDs-Cu^{2+} interactions activate two ultrafast decay channels of the fluorescence and, importantly, their time scales (0.21 ps and 1.9 ps) match those of CD surface solvation, or otherwise more than two time constants would be needed to reproduce data in Figure 4. This coincidence is indeed unexpected and leads to presume a key role of solvation in the quenching process, discussed in detail in the last paragraph.

Finally, our data lead to some further, interesting considerations on the nature of CD/ion complexes involved in static quenching. In fact, the amplitude of the ultrafast fluorescence decay components grow with copper concentration, while the time constants of these decays are independent of it and are always 0.2 and 1.9 ps, as extracted from fitting the single-wavelength traces at 550 nm. This strongly suggests that the quenching dynamics are due to simple, one dot-one ion complexes. In fact, the coexistence of multiple species of the form CD-$(Cu^{2+})_n$, with variable n,

View Article Online
DOI: 10.1039/C7NR03754F

would lead to multiple time scales, dependent on the number of attached ions, and progressively showing up with increasing copper concentration. This important conclusion is also endorsed by the simple trend of the intensity quenching shown in the inset of Figure 1b, where significant intensity decrease is already observed from the lowest copper concentrations we explored. If the successive, multi-step, binding of several copper ions were needed to quench the luminescence, the observed trend would certainly be more complex, and would show an initial lag phase.

3. The quenching mechanism: solvent-driven electron transfer from CDs to metal ions

Based on the results reported so far, we conclude that stable CD-Cu^{2+} complexes are formed by the chemical interaction of ground-state CDs and Cu^{2+} ions, and their emission quenching likely involves a very efficient electron transfer (ET) towards Cu^{2+} ions. Other common mechanisms of fluorescence quenching appear very unlikely: in particular, both resonance- and Dexter-type energy transfer to the d-d absorption transition of aqueous Cu^{2+} ions around 800 nm should be extremely inefficient because the latter is forbidden and has no spectral overlap with CD emission at 520 nm (Figure S6). Besides, an exciton transfer from the CD to the binding ion would give rise to a characteristic ESA signal in the TA spectra due to the ion in the (d,d) excited state,[37] which does not exist in the pump/probe spectra recorded here, conclusively ruling out this mechanism as a cause of fluorescence quenching. In order to confirm the role of ET, we studied the optical properties of a solution of CDs with two different amounts of Zinc ions (Zn^{2+}).

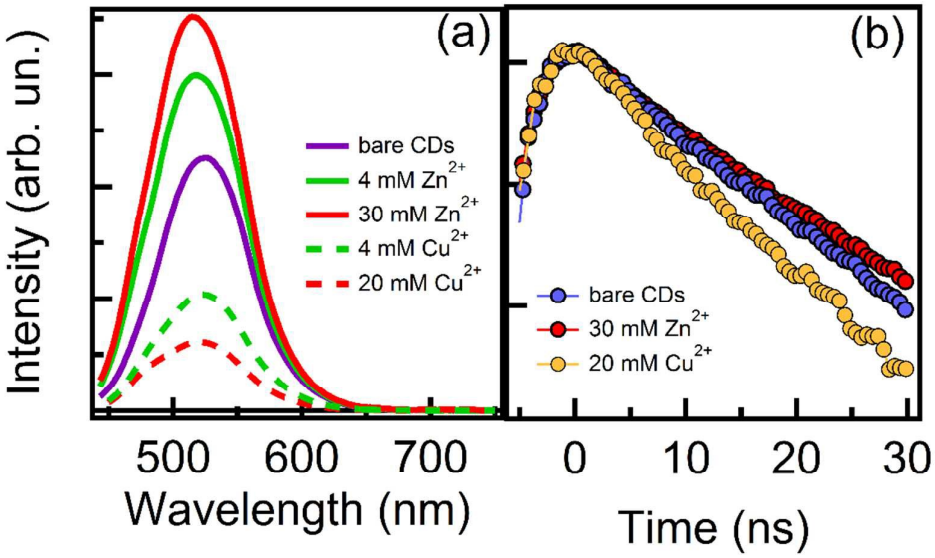

Figure 5: *(a): Emission spectra of a solution of bare CDs dissolved in water (purple) and with different concentration of Zinc and Copper ions. (b): Normalized decay kinetics of the emission band of the solution of bare CDs (purple), of the solution with 30 mM Zn^{2+} (red) and 20 mM Cu^{2+} (orange).*

View Article Online
DOI: 10.1039/C7NR03754F

Because the electronic configuration of Zn^{2+} is $[Ar]3d^{10}$, that is a completely full 3d-shell, no ET is expected with these ions. As shown in Figure 5, the presence of Zn^{2+} in a solution of CDs does not quench the photoluminescence; on the contrary, it causes an increase of the quantum yield, a blueshift of the emission band (Figure 5a) and an extension of the lifetime (Figure 5b), in striking contrast to the effect induced by copper ions. On one hand, this result strongly supports the idea that quenching involves ET from the surface of photo-excited CDs to Cu^{2+} ions; on the other hand, the enhancement of the emission by Zn^{2+} is probably the effect of electrostatic screening provided by Zn^{2+} ions on the negatively-charged surface of CDs (rich of COO- groups). This is expected to reduce the strong solvation effects at CD surfaces, due to dielectric and H-bonding interactions with water, that redshift CD emission and reduce their QYs. [23] Through this mechanism, Zn-induced screening increases the HOMO/LUMO gap and provokes a blueshift of the band, accompanied by an increase of the lifetime and quantum yield of the transition. Additionally, the attached Zn^{2+} may increase QY by limiting geometrical rearrangement of the surface groups that provide non-radiative dissipation channels. In order to better understand the effect of Zn ions, we performed TA measurements on the solution of CDs with 30 mM Zn^{2+}. As shown in Figure S7, the pump/probe signal (Figure S7a) is very similar to the one observed in the solution of bare CDs and, in particular, the kinetics of the SE signal is practically the same (Figure S7b) in both solutions, underlining the absence of any SE decay in presence of zinc ions. On the other hand, we noted, in presence of Zn^{2+}, a smaller solvatochromic shift of the SE than in pure water (at t>10 ps, the SE peaks at 556 nm for CDs in pure water and at 550 nm in presence of Zn^{2+}) which confirms the screening effect discussed above and the following enhancement of the emission. Even in the case of Cu^{2+}, when an ET mechanism is viable, ultrafast fluorescence quenching may coexist with a screening mechanism similar to that induced by Zn^{2+}. Such an effect may contribute to the blueshift of the steady-state emission observed in Figure 1b.

We recently developed a model for the lowest electronic transitions of these CDs, [23] in which optical absorption has a certain core-to-surface charge transfer character: in particular, the transition causes an increase of electronic charge on surface carboxylic and amide groups, occupying their π^* empty orbitals, and leaves a hole which mostly resides on C_3N_4 core atoms in proximity of the surface. Both carboxylic and amide groups, common on the surface of many CDs, are potential anchoring sites of Cu^{2+} ions, as reported in previous studies, [8,11] and in particular N-containing groups, as amide, seem to have a special binding affinity to Cu^{2+}. [11,13] Considering this, and bearing in mind the possible role of the surface groups in the photocycle, we performed infrared (IR) absorption measurements on bare CDs and on a sample of CDs after addition of copper nitrate. We observe small, but appreciable variations in the region between 1550-1800 cm^{-1}, associated to

View Article Online
DOI: 10.1039/C7NR03754F

vibrations of amide and carboxylic surface groups, [29] such as a blueshift of the amide II vibration (Figure S8). Although the observed changes are too complex to infer a simple binding pattern, IR data seem to confirm that these surface groups are involved in the formation of the complexes between Cu^{2+} and CDs.

On these grounds, we expect a very close proximity of the photo-excited surface electron to the acceptor Cu^{2+} ion, and a very strong coupling between the Franck-Condon (FC) state, and the ET state, consistent with the ultrafast electron transfer we observe. However, the mixing between the FC and the ET states must be initially rather small, since the initial excited state is very close to the FC state of the bare CDs, as revealed by: i) the fact that the shape of the SE at time zero is essentially unchanged in presence of Cu^{2+} (Figure 3c and 3d); ii) by the independence of the extrapolated SE signal amplitude at time zero from copper concentration (Figure S9), indicating that the nature of the initially excited state is independent of the presence of copper. The preservation of the FC state requires the existence of a defined barrier separating it from the ET state, as represented by the double-well potential energy surface in Figure 6. On the other hand, our finding that ET occurs bi-exponentially on the same time scales (0.21 and 1.9 ps), that characterize aqueous solvation on bare CDs, rules out a direct through barrier transition from the FC to the ET states, since it would imply new decay components in the fitting procedure. Conversely, it speaks for an adiabatic ET process driven by solvent rearrangement. Thus we propose that solvation progressively decreases the barrier between the FC state and the ET state (see Figure 6) until the charge transfer is allowed and decouples the surface electron from the core hole, depopulating the emissive state. An adiabatic process implies a continuously-changing degree of mixing of the FC and ET states during the reaction, rather than an abrupt change of the electronic wavefunction. The idea of an adiabatic ET from CDs to Cu^{2+} is consistent with the small variation of the optical absorption spectra displayed in Figure 1a: a small mixing between the FC state and the ET state, already existing at the time of photo-excitation, will increase the core-to-surface charge transfer character of the transition, and lower its oscillator strength, explaining the reduction of the absorption intensity.

After initial photo-excitation, solvent rearrangement drives the ET reaction towards Cu^{2+} to its completion. A deep involvement of solvent relaxation in this reaction is actually expected: in fact, the photo-induced change of the surface charge distribution, directly exposed to the solvent, is expected to trigger a dramatic solvent rearrangement, as observed in similar cases. [38] The solvent reaction goes always in the direction to stabilize solvated charges. This implies that in its characteristic time scales, solvent rearrangement will lower the barrier that keeps the charge on the photo-excited CD. This will also facilitate the first step of the ET process and trigger the

View Article Online
DOI: 10.1039/C7NR03754F

progressive population of Cu^{2+} empty d-shell. In a cooperative way, this is expected to promote a further, strong solvent rearrangement as the reaction proceeds, because Cu^{2+} and Cu^{+} ions are characterized by completely different aqueous solvation shells (octahedral vs tetrahedral). [39] As a consequence of such a solvent-controlled mechanism, the time required for water rearrangement limits the efficiency of ET notwithstanding a strong coupling. In fact, in other cases ET can be much faster than observed here: Williams et al. reported a time scale well below 100 fs for the electron injection from photo-excited graphene quantum dots to TiO_2 nanoparticles, in one of the few available studies on these systems. [16]

The last step of the photocycle involves the transition of the CD-Cu^{2+} system back to the ground state. In this respect, Figure 3 shows that the ultrafast SE decay is accompanied by the disappearance of all the other components of the TA signal. The decay of the GSB on the same time scale, in particular, implies an extremely fast repopulation of the ground state immediately after ET. To be consistent with the data, the ground-state recovery must be much faster than 1 ps (or otherwise the GSB would disappear later than the SE), and cannot be directly observed here because the time scale τ_2 is a bottleneck of the overall dynamics. The nature of this final step is ultimately a back electron transfer inducing a non-radiative electron-hole recombination. A sub-ps timescale suggests that the recombination is likely mediated by a sequence of inelastic electron-phonon scattering processes, usually allowing to dissipate large excess energies within 100s of femtoseconds. [40] This process completes the photo-cycle and hinders steady-state emission from CDs-Cu^{2+} complexes. The $e^{-}h^{+}$ pair recombination time here observed is definitively faster than what reported in other CD complexes with different oxidizing agents. [41] An important effect of the chosen oxidizing agent is very probable but no specific study on this issue has been published yet. We can guess that the crucial step is the reinjection of the electron into the CD, while the dissipation of the Coulomb energy should be similar to what here observed.

Finally, the fast reverse process suggests that the ET reaction is only partial, or otherwise the complete loss of the electron-hole overlap would render non-radiative recombination relatively inefficient. Indeed, within the model in Figure 6, the final state produced by the ET reaction can be more realistically pictured as one where the electron has become completely delocalized between the surface group and the metal ion, rather than a state where the electron has been fully transferred from the surface carboxylic/amide group to the nearby Cu^{2+}.

View Article Online
DOI: 10.1039/C7NR03754F

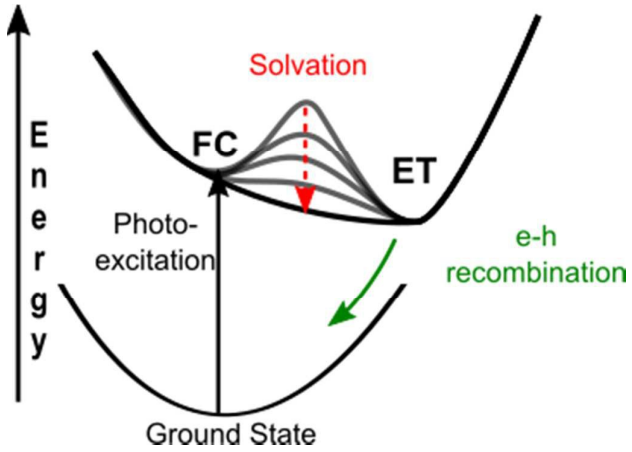

Figure 6: *Model which represents the photo-cycle of CDs-Cu^{2+} complexes. After photoexcitation, an exciton is formed and the system is in an electronic state (FC) which relaxes due to solvent motions in 0.21 + 1.9 ps (red arrow) and causing a partial electron transfer from the CD to Cu^{2+}. The cycle is closed by an ultrafast non-radiative electron-hole recombination (<<1 ps, green arrow).*

Conclusions

The combined use of steady-state, nanosecond-time-resolved and femtosecond optical spectroscopies provided a detailed picture of the dynamics responsible of CD fluorescence quenching by transition metal ions, from the femtosecond to the nanosecond time range. Most CDs are efficiently quenched by Cu^{2+} ions through the formation of stable CD-Cu^{2+} complexes, wherein an ion directly binds to surface amide and/or carboxylic groups closely involved in the photoexcitation mechanism of the dot A minority of CDs are quenched by a collisional mechanism, reflecting in variations of their nanosecond decay kinetics. In both cases, quenching involves an electron transfer mechanism which is unviable for closed d-shell ions such as Zn^{2+}. We additionally find that both static and dynamic quenching are affected by heterogeneity in the reaction rates, giving rise to photoselection effects. The study of CD-Cu^{2+} complexes by ultrafast spectroscopies reveals the characteristic time scales and mechanism of the ET dynamics, which turn out to be 0.21 ps and 1.9 ps. Our data strongly suggest that the ET process is only partial, and mostly controlled by a strong, and very fast, solvent rearrangement around the dot, initiated by photo-excitation, and driving a progressive reduction of the barrier for the ET reaction. The photocycle of CDs is completed by a fast, non-radiative recombination of the electron-hole pair, likely mediated by a cascade of inelastic electron-phonon scattering processes. Such a comprehensive view of electron transfer dynamics involving photoexcited carbon nanodots may help tailoring their properties to advance the design of photoactive, CD-based nanoscale materials.

View Article Online
DOI: 10.1039/C7NR03754F

Acknowledgments

We thank the LAMP group (www.unipa.it/lamp) at University of Palermo for support and stimulating discussions. We thank Prof. Valeria Vetri for our use of optical spectroscopy facilities in her laboratory. We acknowledge financial support received by project "MedNETNA-Mediterranean Network for emerging nanomaterials" (P.O. F.E.S.R. 2007/2013 – line 4.1.2.A).
Steady State photoluminescence and infrared measurements were carried out at the optical spectroscopy laboratory of ATeN center – CHAB, and single-wavelength TA measurements and some of the broadband TA measurements were carried out at the UFL laboratory of ATeN center – CHAB (http://www.atencenter.com). AC gratefully acknowledges the ERC Starting Grant 279599-FunctionalDyna) and Swiss NSF through the NCCR MUST "Molecular Ultrafast Science and Technology" for the financial support.

References

1. X. Xu, R. Ray, Y. Guy, H.J. Ploehn, L. Gearheart, K. Raker and W.A. Scrivens, *J. Am. Chem. Soc.*, 2004, **126**, 12736-12737.

2. Y.-P. Sun, B. Zhou, Y. Lin, W. Wang, K.A. Fernando, P. Pathak, M.J. Meziani, B.A. Harruff, X. Wang, H. Wang, P.G. Luo, H. Yang, M. Kose , B. Chen, L.M. Veca et al., *J. Am. Chem. Soc.*, 2006, **128**, 7756-7757.

3. S.-T. Yan, X. Wan, H. Wang, F. Lu, P.G. Luo, L. Cao, M.J. Meziani, J.-H. Liu, Y. Liu , M. Chen, Y. Huang and Y.-P.Sun, *J. Phys. Chem. C*, 2009, **113**, 18110-18114.

4. H. Peng and J. Travas-Sejdic, *Chem. Mater.*, 2009, **21**, 5563-5565.

5. P. Miao, K. Han, Y. Tang, B. Wang, T. Lin and W. Cheng, *Nanoscale*, 2015, **7**, 1586.

6. A. Zhu, Q. Qu, X. Shao, B. Kong and Y. Tian, *Angew. Chem. Int. Ed.*, 2012, **51**, 7185 – 7189.

7. L. Zhou, Y. Lin, Z. Huang, J. Ren and X. Qu, *Chem. Commun.*, 2012, **48**, 1147–1149.

8. J. Zong, X. Yang, A. Trinchi, S. Hardin, I. Cole, Y. Zhu, C. Li, T. Muster and G. Wei, *Biosens. Bioelectron.*, 2014, **51**, 330-335.

9. Y.-L. Zhang, L. Wang, H.-C. Zhang, Y. Liu, H.-Y. Wang, Z.-H. Kang and S.-T. Lee ST, *RSC Adv.*, 2013, **3**, 3733–3738.

10. M. Vedamalai, A.P. Periasamy, C.-W. Wang, Y.-T. Tsen, L.-C. Ho, C.-C. Shih and H.-T. Chang, *Nanoscale*, 2014, **6**, 13119-13125.

11. S. Zhang, J. Li, M. Zeng, J. Xu, X. Wang and W. Hu, *Nanoscale*, 2014, **6**, 4157-4162.

View Article Online
DOI: 10.1039/C7NR03754F

12. F. Wang, Z. Gu, W. Lei, W. Wang, X. Xia and Q. Hao, *Sens. Actuators B*, 2014, **190**, 516-522.

13. Y. Dong, R. Wang, G. Li, C. Chen, Y. Chi and G. Chen, *Anal. Chem.*, 2012, **84**, 6220-6224.

14. X. Wang, L. Ca, F. Lu, M. Meziani, H. Li, G. Qi, B. Zhou, B.A. Harruff, F. Kermarrec and Y.-P. Sun, *Chem. Commun*, 2009, 3774–3776.

15. S. Mondal, S.K. Seth, P. Gupta and P. Purkayashta, *J. Phys. Chem. C*, 2015, **119**, 25122-25128.

16. K.J. Williams, C.A. Nelson, X. Yan,L.-S. Li and X. Zhu, *ACS Nano*, 2013, **7**, 1388-1394.

17. X. Yan, X. Cui, B. Li and L.-S. Li, *Nano Lett.*, 2010, **10**, 1869–1873.

18. H. Ming, Z. Ma, Y. Liu, K. Pan, H. Yu, F. Wang and Z. Kan, *Dalton Trans.*, 2012, **41**, 9526–9531.

19. X. Yu, J. Liu, Y. Yu, S. Zuo and B. Li, *Carbon*, 2014, **68**, 718-724.

20. H. Li, R. Liu, Y. Liu, H. Huang, H. Yu, H. Ming, S. Lian, S.-T.Lee and Z. Kang, *J Mater Chem*, 2012, **22**, 17470–17475.

21. B.Y. Yua and S.-Y. Kwak, *J. Mater. Chem.*, 2012, **22**, 8345-8353.

22. H. Zhang, H. Ming, S. Lian, H. Huang, H. Li, L. Zhang, Y. Li, Z. Kang and S.-T. Lee, *Dalton Trans.*, 2011, **40**, 10822-10825.

23. A. Sciortino, E. Marino, B. van Dam, P. Schall, M. Cannas and F. Messina, *J. Phys. Chem. Lett.*, 2016, **7**, 3419-3423.

24. D.A. Hines and P.V. Kamat, *ACS Appl. Mater. Interfaces*, 2014, **6**, 3041-3057.

25. H. Kang, K. Lee, B. Jung, Y.J. Ko and S.K. Kim, *J. Am. Chem. Soc.*, 2002, **124**, 12958-12959.

26. P. Yu, X. Wen, Y.-R. Toh, Y.-C. Lee, K.-Y. Huang , S. Huang, S. Shrestha, G. Conibeer and J. Tang, *J. Mater. Chem. C*, 2014, **2**, 2894-2901.

27. X. Wen, P. Yu, Y.-R. Toh, X. Hao and J. Tang, *Adv. Opt. Mater.*, 2013, **1**, 173-178.

28. l. Wang, S.-J. Zhu, H.-Y. Wang, S.-N. Qu, Y.-L. Zhang, J.-H. Zhang, Q.-D. Chen, H.-L. Xu, W. Han, B. Yang and H.-B. Sun, *ACS Nano*, 2014, **8**, 2541–2547.

29. F. Messina, L. Sciortino, R. Popescu, A.M. Venezia, A. Sciortino, G. Buscarino, S. Agnello, R. Schneider, D. Gerthsen, M. Cannas and F.M. Gelardi, *J. Mater. Chem C*, 2016, **4**, 2598-2605.

30. R. Lakowicz, Principles of Fluorescence Spectroscopy: Springer Science; 2006.

31. C. Reichardt, *Chem. Rev.*, 1994, **94**, 2319-2358.

View Article Online
DOI: 10.1039/C7NR03754F

32. G.R. Fleming, *Annu. Rev. Phys. Chem.*, 1996, **47**, 109-134.

33. S. Khan, A. Gupta, N.C. Verma and C.K. Nandi, *Nano Lett.*, 2015, **15**, 8300-8305.

34. D. Pant and N. E. Levinger, *Chem. Phys. Lett.*, 1998, **292**, 200-206.

35. O. Braem, A. Ajdarzadeh Oskouei, A. Tortschanoff, F. van Mourik, M. Madrid, J. Echave, A. Cannizzo and M. Chergui, *J. Phys. Chem. A*, 2010, 114, 9034-9042.

36. J. Peon, S. K. Pal and A. H. Zewail, *Proc. Natl. Acad. Sci. USA,* 2002, **17**, 10964-10969.

37. J. Rodriguez and D. Holten, *J. Chem. Phys*., 1989, **91**, 3525-3531

38. F. Messina, O. Braem, A. Cannizzo and M. Chergui, *Nat. Commun.*, 2013, **4**, p. 2119.

39. I. Persson, *Pure Appl. Chem.*, 2010, **82**, 1901-1917.

40. F. Carbone, G. Aubock, A. Cannizzo, F. Van Mourik, R.R. Nair, A.K. Geim, K.S. Novoselov and M. Chergui, *Chem. Phys. Lett.*, 2011, **504**, 37-40.

41. V. Strauss, J.T. Margraf, C. Dolle, B. Butz, T.J. Nacken, J. Walter, W. Bauer, W. Peukert, E. Spiecker, T. Clark and D.M. Guldi, *J. Am. Chem. Soc.*, 2014, **136**, 17308-17316.